

**237. The Production of Active Solids by Thermal Decomposition.**  
*Part XI.<sup>1</sup> The Heat Treatment of Precipitated Stannic Oxide.*

By J. F. GOODMAN and S. J. GREGG.

Two batches of stannic oxide gel have been prepared, batch A virtually ion-free by the hydrolysis of stannic ethoxide and batch B by precipitating aqueous stannic chloride with aqueous ammonia. Separate samples of each batch were heated for five hours at a series of fixed temperatures in the range 25—1600° (batch A) or 25—1000° (batch B), and various properties of the cooled product were then determined. These include the specific surface by nitrogen adsorption; pore volume and average pore diameter by adsorption of the vapours of methanol and of carbon tetrachloride and by density measurements; the X-ray and electron diffraction pattern and the electron micrograph. Each batch shows a continuous decline of specific surface as the temperature of calcination is increased, but the pore volume of batch A varied only slightly between 25° and 1500°, indicating a very stable gel structure. Batch B, on the other hand, showed a sharp increase in pore volume between 400° and 500°, owing to the expulsion of contaminating stannous chloride. The loss of specific surface for batch A becomes faster near 1100°, which probably marks the Tammann temperature, and suggests that the melting point of stannic oxide is *ca.* 2500°.

THE calcination of precipitated silica, discussed in Part X,<sup>1</sup> exhibits somewhat unusual characteristics and it was considered worthwhile to subject precipitated stannic oxide to a corresponding examination. Stannic oxide might be expected to show some similarities to silica (in view of the rather close chemical relation between the two oxides), and yet certain differences also, since SnO<sub>2</sub>, unlike the amorphous SiO<sub>2</sub>, is crystalline even at low temperatures. At the same time the opportunity was taken to study the effect of ions present during precipitation, by preparing one sample of stannic oxide under virtually ion-free conditions (as in Part X<sup>1</sup> for silica) and another in the presence of a significant concentration of ions.

## EXPERIMENTAL

*Materials.*—The first, "ion-free," sample of stannic oxide (batch A) was obtained by the hydrolysis of stannic ethoxide. A solution made by dissolving freshly distilled stannic chloride in dried absolute alcohol was added dropwise to an equivalent quantity of sodium ethoxide also dissolved in absolute alcohol, and the mixture refluxed for 30 hr.; the precipitated sodium chloride was removed by rapid filtration, and the solution poured into a large excess of distilled water. After a few hours the supernatant liquid was siphoned off and distilled water added. The siphoned liquid contained a small quantity of chloride ions; this was expected since sodium chloride is slightly soluble in alcohol. The precipitate was washed several times with distilled water, filtered, air-dried at 25°, and broken into lumps. Although there may be a trace of ionic impurity in this sample (due to contamination with sodium chloride), for the present purposes it may be considered virtually ion-free.

Batch B, the ion-contaminated sample, was prepared from stannic chloride by precipitation with aqueous ammonia. Precipitation was carried out in three large tanks, each containing an excess of distilled water. Equal quantities of 1.2*N*-ammonia and of 1.0*N*-stannic chloride were run separately into each tank from two aspirators, vigorous stirring being maintained during the precipitation. The gel was allowed to settle overnight, then the supernatant liquid was siphoned off and the sludges were transferred to a single tank. After being washed several times with distilled water the precipitate was filtered off and air-dried at 15°. The gel was crushed to obtain a sample in which the ionic impurities were evenly distributed.

On thermogravimetric analysis<sup>2</sup> batch A, like silica, gave results corresponding to the loss of adsorbed water only, with a single peak at *ca.* 200° in the curve of  $\Delta W/\Delta T$  against  $T$  ( $W$  = weight of sample,  $T$  = temperature). In contrast batch B, the ion-contaminated sample,

<sup>1</sup> Part X, Goodman and Gregg, *J.*, 1959, 694.

gave, in addition, subsidiary peaks at 350° and 550°; chemical analysis suggested that the peak at 350° was caused by the loss of ammonium chloride, and that at 550° by the loss of stannous chloride formed presumably by the decomposition of a basic stannic chloride. Batch A, therefore, consists of a pure hydrous oxide, whilst batch B is contaminated with ammonium chloride and a basic stannic chloride. The results gave no evidence for a stoichiometric hydrate in either batch, confirming the view that the so-called "stannic acids" are, in fact, stannic oxide containing adsorbed water.

*Procedure.*—Portions of each batch were heated for 5 hr. each at a fixed temperature within the range 25–1600°. The "water" content,  $w$ , corresponding to each temperature of calcination was obtained by repeating the calcination with a separate portion of the starting material, then raising the temperature to 1000° and keeping it there until constant weight was obtained, as registered on the thermal balance. The properties of the cooled product were determined by procedures previously outlined (Parts IX<sup>2</sup> and X<sup>1</sup>): (i) Specific surface by nitrogen adsorption<sup>3</sup> at –183°; (ii) sorption isotherms at 22° of methanol and of carbon tetrachloride; (iii) apparent density by displacement in mercury,<sup>2</sup>  $\rho_{Hg}$ , and in carbon tetrachloride<sup>5</sup>  $\rho_{CCl_4}$ ; (iv) X-ray and electron diffraction patterns and the electron micrograph.<sup>1</sup> The electron diffraction patterns were obtained from selected areas of the electron micrograph, the intermediate aperture being used to isolate a circular area *ca.* 0.8 micron in diameter. For samples heated at the higher temperatures (above *ca.* 500°) individual crystals could be identified unambiguously by selecting diffraction spots with the objective aperture for the dark-field micrograph. Finally, a portion of the starting material of each batch was examined dilatometrically. A compact was made by compressing the crushed gel, and the length of the compact was followed with a simple extensometer<sup>2</sup> while the temperature was raised at 200°/hr. Its volume was calculated on the assumption that it shrinks isotropically.

## RESULTS

We report first the results for pure stannic oxide (batch A). The specific surface diminishes continuously with increasing temperature of calcination, apart from a small rise at the low temperature end of the curve (Fig. 1, Curve I); correspondingly the average crystallite length  $l$

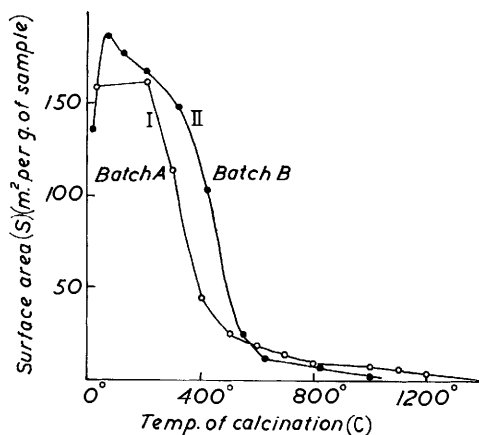


FIG. 1. Plot of surface area  $S$  (in  $m.^2$  per g. of sample) of calcined stannic oxide against temperature of calcination.

(calculated as  $l = 6/\rho S$  where  $\rho$  is the true density and  $S$  is the specific surface per g. of solid material) increases as the temperature of calcination increases. This growth in crystallite size is confirmed by the X-ray and the electron optical results. The X-radiograms show an increasing sharpness of the cassiterite pattern as the calcination temperature increases; the selected area diffraction patterns are, for the 200° and 300° samples, continuous rings consistent with aggregates of small crystals; at 500° they are composed of spots; and at higher temperatures the patterns represent the superposition of the patterns of a few individual crystallites.

<sup>2</sup> Goodman and Gregg, *J.*, 1956, 3612.

<sup>3</sup> Gregg, *J.*, 1953, 3940.

<sup>4</sup> Pierce *et al.*, *J. Phys. Chem.*, 1949, **53**, 669; 1953, **57**, 64.

<sup>5</sup> Cottrell, "Dislocations and Plastic Flow in Crystals," Clarendon Press, Oxford 1953, Chapter V.

In the electron micrographs (see Plate) taken with the dark-field technique, individual crystallites could be distinguished and their average linear dimension  $\delta$  estimated; the values of  $l$  and  $\delta$  were in satisfactory accord (Table 1).

TABLE 1. Crystallite size ( $\text{\AA}$ ) and volume to surface ratio ( $\text{\AA}$ ).

Temp. ....	200°	300°	500°	800°	1100°	1200°	1350°	1400°
$l$ .....	66	82	337	880	1400	2610	—	10,900
$\delta$ .....	—	15—80	50—300	100—600	400—1500	—	1000—6000	—
$V/10^4S$ .....	4.9	8.2	42	115	—	300	1500*	—

\* At 1400°.

$l$  = Crystallite length from  $l = 6/\rho S$ .  $\delta$  = Crystallite length from electron micrograph.  $V$  = Pore volume, cm.<sup>3</sup> per g. of sample.  $S$  = Specific surface, m.<sup>2</sup> per g. of sample.

TABLE 2. Stannic oxide, batch A. Dependence of specific surface on time of outgassing.

Temp. (°c)	25°	25°	25°	105°	105°	105°	105°	105°	105°	200°
Time (hr.)	1	5	20	1	5	20	67	229	487	5
$S'$ .....	171	175	174	125	150	163	163	163	163	172
$w$ .....	11.0	9.6	9.0	12.8	9.8	8.0	7.6	7.4	7.1	5.2

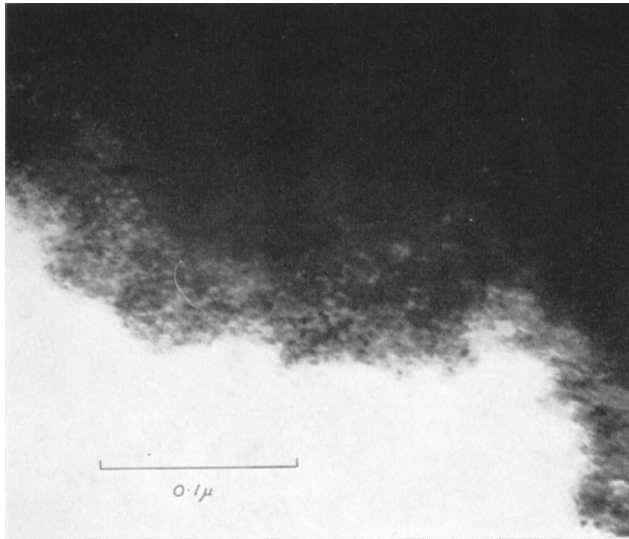
$S'$  = Surface area in m.<sup>2</sup> per g. of SnO<sub>2</sub>.  $w$  = Water content, g. per 100 g. of SnO<sub>2</sub>.

The initial rise in curve I is probably a reflection of the marked dependence of the measured specific surface on the conditions of outgassing. As is seen from Table 2, the specific surface at first increases with time of outgassing at both 25° and 105°, probably because of the removal of water from the finest pores, whereby surface which was previously covered or inaccessible becomes exposed. After a time, however, the surface fails to increase further even though the water content is falling; and this suggests that the increase in surface which should be brought about by loss of water is now being outweighed by a loss of area due to sintering (Part I<sup>3</sup>). The actual value obtained for specific surface will thus depend on such factors as the water content before outgassing, and the initial maximum of curve I is therefore probably devoid of particular significance.

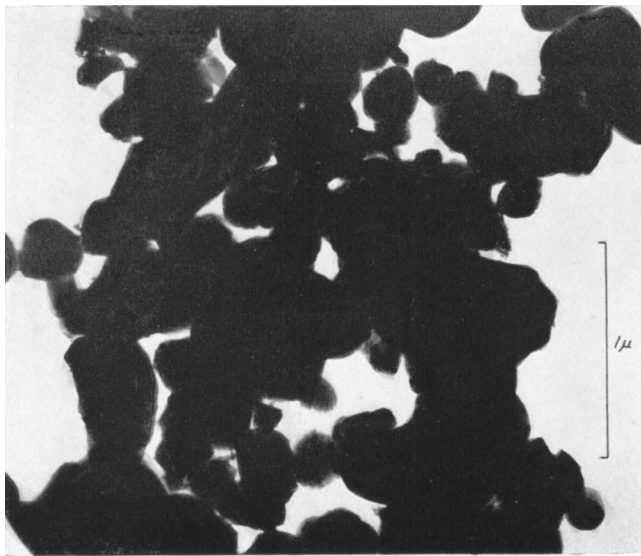
The pore volume  $V$  was calculated both as the difference ( $1/\rho_{\text{Hg}} - 1/\rho_{\text{CCl}_4}$ ), and by application of the Gurwitsch relation to the carbon tetrachloride isotherms; the values by the two methods agree reasonably well (<5%) for any given sample (cf. Part X<sup>1</sup>). In contrast to the specific surface, the pore volume and correspondingly the lump volume ( $=1/\rho_{\text{Hg}}$ ) undergo remarkably little alteration with change in temperature below 1500°. The ratio  $V:S$  must therefore increase extensively as temperature of calcination increases, so that the average pore width [ $\propto(V/S)$ ]<sup>2</sup> must likewise increase; and the pore-size distribution, since  $V$  is nearly constant, must alter in favour of the larger pores. The forms of the adsorption isotherms are in accord with this: the type I isotherm obtained with low-temperature samples (Fig. 3 and 4) is characteristic of adsorbents having pores of molecular dimensions;<sup>4</sup> as temperature of calcination increases, type IV isotherms indicative of larger pores are obtained and the hysteresis loop moves towards high pressures, denoting an increase in the average pore diameter  $d$ . The value of  $d$  calculated as  $d = 4V/S$  (cylindrical pores thus being assumed<sup>1</sup>) is in broad agreement with the size of the interstices between the crystallites estimated from the electron micrographs. For example, pores of molecular dimensions (20—40  $\text{\AA}$ ) can be clearly distinguished in the micrograph of the 300° sample (Plate), in good agreement with the value of  $d = 35 \text{\AA}$  calculated from the  $V:S$  ratio. Similarly, the 1350° sample shows pores of irregular shape, having widths between about 1000 and 5000  $\text{\AA}$  as compared with the  $V:S$  ratio of 1500  $\text{\AA}$ , or the value of  $d = 6000 \text{\AA}$  for cylindrical pores.

Calcination of the ion-contaminated sample (batch B) covered a smaller range of temperature but the curve for specific surface is qualitatively similar to that for batch A except that the peak at the low-temperature end is more pronounced. The results for volume showed a marked difference, however, for in the region of 400—500°, where according to the thermogravimetric analysis stannous chloride is being driven off, both the lump and the pore volume (Fig. 2) show a large and sudden increase to a high value which diminishes irregularly and slowly with rise in temperature.

*Electron micrographs of ion-free stannic oxide (batch A) calcined at (a) 300°, (b) 1350° c.*



(a)



(b)

*In (a) crystallites 15—80 Å long and pores 20—40 Å across can be distinguished; and in (b) crystallites 1000—6000 Å long and pores 1000—5000 Å across.*

[To face p. 1164.]

The sharp increases in lump volume and in pore volume corresponded to a marked change in the physical appearance of the material: the sample heated to 420° still had its original appearance of discrete gel fragments, but the sample heated to 520° was transformed into a single lump moulded into the bottom of the test tube used for its preparation.

FIG. 2. Plot, for calcined stannic oxide, of (a) lump volume, (b) pore volume from density data, against temperature of calcination.

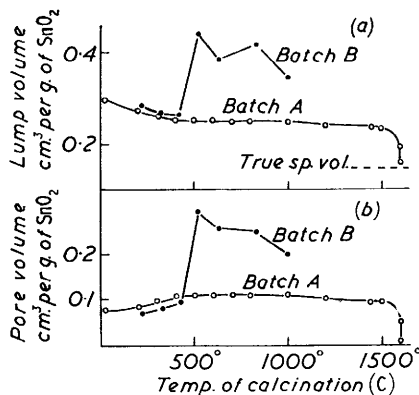


FIG. 3. Sorption isotherms at 22° of carbon tetrachloride vapour on ion-free stannic oxide (batch A) calcined at different temperatures. The temperature of calcination is marked on each isotherm. Tails denote desorption points.

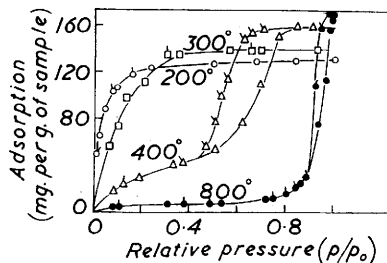
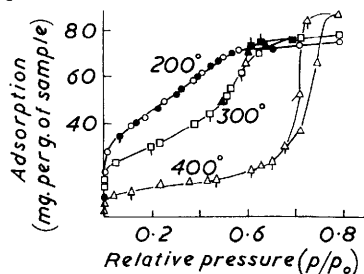


FIG. 4. Sorption isotherms at 22° of methano vapour on ion-free stannic oxide (batch A) calcined at different temperatures. The temperature of calcination is marked on each isotherm. Tails denote desorption points.



300° sample. □ First sorption cycle; ■ second sorption cycle; ▲ third sorption cycle.

DISCUSSION

The results for batch A will be discussed first. The diminution in specific surface with increase in temperature of calcination is similar to that found with ferric oxide<sup>2</sup> and with silica<sup>1</sup> and is consistent with the fact that stannic oxide gel is a hydrous oxide; as there is no change in lattice when the water is driven off, a rise in the temperature of calcination produces sintering but not activation,<sup>3</sup> and the area thus shows only a tendency to decrease. (The small rise at the low-temperature end has already been explained.)

Perhaps the most striking feature of the results is that the large decrease in specific surface between 100° and 1450° from 163 to 0.8 m.<sup>2</sup> g.<sup>-1</sup> is accompanied by an almost negligible change in pore volume and in lump volume. The growth in crystallite size responsible for the reduction in specific surface must occur in such a way as to alter the pore-size distribution in favour of the larger pores without significantly altering either the total volume of the pores or the overall volume of each grain, the volume of the small pores as they are eliminated being added to that of larger ones. This kind of behaviour can be explained if there are some crystallites whose growth is favoured at the expense of

their neighbours. Such crystallites would presumably be those which have the lowest strain energy and are suitably oriented so that adhesion to neighbours occurred through large-angle grain boundaries, growth involving plastic flow across the grain boundaries<sup>5</sup> by the movement of dislocations.

By analogy with other systems (*e.g.*, the gels of ferric oxide,<sup>2</sup> silica,<sup>1</sup> alumina,<sup>6</sup> titania<sup>7</sup>) acceleration of the sintering process might be expected at a temperature near  $0.5T_m$  ( $T_m = \text{m. p. in } ^\circ\text{K}$ ).<sup>8</sup> Reference to Fig. 5 shows that at *ca.* 1100° an accelerated loss of area does indeed occur. Unfortunately the melting point of  $\text{SnO}_2$  is unknown and the best data available indicate only that it lies above 2200°K.<sup>9</sup> If we accept the view that the accelerated loss of area at about 1100°C marks  $0.5T_m$  then the melting point will be *ca.* 2750°K. It is interesting that many reference books incorrectly list the m. p. of  $\text{SnO}_2$  as 1127°, approximately the temperature which marks the accelerated sintering process.

In the region 300–500° the rate of loss of surface area first seems to accelerate and then to decelerate somewhat as the temperature rises. This feature may well be connected with the fact that a small reversible crystallographic change from the alpha- to the beta-form of cassiterite is believed to occur at 425°;<sup>10</sup> the occurrence of this transformation implies an enhanced mobility in this temperature region.

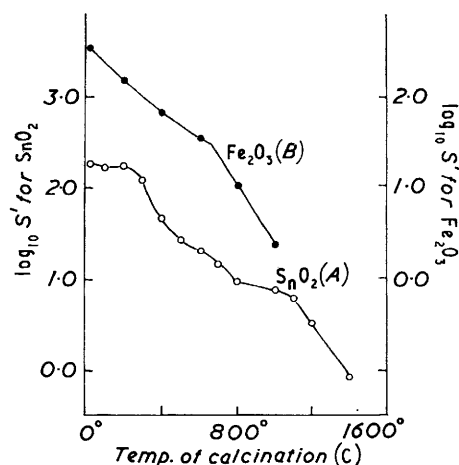


FIG. 5. Plot of  $\log S'$  against calcination temperature for stannic oxide (batch A) and ferric oxide (batch B).<sup>1</sup> ( $S'$  = surface area in  $\text{m}^2$  per g. of  $\text{SnO}_2$  or of  $\text{Fe}_2\text{O}_3$ .) For  $\text{SnO}_2$  use left-hand, for  $\text{Fe}_2\text{O}_3$  use right-hand, scale.

Despite the accelerated loss of surface area above 1100°, it is only at 1550–1600° that the pore volume suddenly falls to zero (within the limits of experimental error), showing that the gel structure collapses at a temperature much in excess of  $0.5T_m$ . Analogous behaviour is found with ferric oxide gel batch B, where the gel structure was observed to collapse at 1000–1100°, although accelerated loss in surface area was observed above  $0.5T_m$  for this gel also.\* With several other oxides however (*e.g.*, alumina,<sup>6</sup> silica,<sup>1</sup> titania,<sup>7</sup> some samples of ferric oxide,<sup>2</sup> and probably magnesia<sup>11</sup>) a rapid fall in both pore volume and surface area occurs in a range of temperature close to  $0.5T_m$ . (With many oxides it is probable that sealed-off pores remain which can only be removed by very prolonged heating at temperatures near the melting point.<sup>12</sup>) The difference in behaviour

\* The point for the 600° sample of ferric oxide (batch B; Part IX) was incorrectly plotted. The correct curve is plotted for comparison with  $\text{SnO}_2$  in Fig. 5 of this paper where the sudden change in slope near 650° is seen. For ferric oxide  $0.5T_m \approx 660^\circ$ .

<sup>6</sup> Gregg and Wheatley, *J.*, 1955, 3804.

<sup>7</sup> Asher and Gregg, also Gregg and Pope, unpublished work.

<sup>8</sup> Finch and Sinha, *Proc. Roy. Soc.*, 1957, *A*, 239, 145.

<sup>9</sup> Brewer, *Chem. Rev.*, 1953, 52, 1.

<sup>10</sup> Laschenko and Kompananskii, *J. Appl. Chem. (U.S.S.R.)*, 1935, 8, 628.

<sup>11</sup> Gregg and Packer, *J.*, 1955, 51.

<sup>12</sup> Bourke, *J. Amer. Ceram. Soc.*, 1957, 40, 80.

of different oxides is not altogether surprising: the ease with which the framework of a particular gel can collapse would depend, not only on the mobility of its constituent ions, but also on such factors as the shape and relative orientation of the sol particles in the original gel, and the rate at which the temperature is raised;<sup>2</sup> these factors can vary widely according to the chemical nature of the gel, the mode of its preparation, and its subsequent treatment.

The main feature of interest with the ion-contaminated material (batch B) is the marked increase in lump volume and in pore volume (Fig. 2) which accompanies the expulsion of the ionic impurity, probably stannous chloride. The increase is a natural consequence of the cementing together of the gel fragments, which has already been referred to; for the mercury used in determining the density for calculation of pore volume (vapour-adsorption isotherms were not measured for batch B) could not penetrate between the gel fragments; but why such a cementing effect should accompany the loss of volatile impurity is not clear. One possibility is that high internal gas pressures are set up which press neighbouring crystallites together and so promote their adhesion.

*Conclusion.*—Stannic oxide shows more resemblances to other crystalline oxides than to silica in its sintering behaviour. The peculiarities observed with silica may therefore be ascribed to its amorphous character (Part X).<sup>1</sup>

For ion-free stannic oxide, calcination results in a growth of wide pores at the expense of narrow, without a significant change in pore volume below *ca.* 1550°. The loss of surface area and the crystal growth which accompany this process possibly occur by the adhesion of crystallites under the influence of surface forces, involving plastic flow across the grain boundaries by the movement of dislocations. The accelerated loss in specific surface observed at 1100° is believed to mark the Tammann temperature ( $\sim 0.5T_m$ ), indicating that the melting point,  $T_m$ , of stannic oxide is *ca.* 2500°.

The temperature, 1550°, at which the pore volume begins to diminish, is well above  $0.5T_m$ , showing that the gel structure of the ion-free stannic oxide specimen used for this investigation is exceptionally stable. On the other hand, the loss of impurity from the ion-contaminated sample of stannic oxide caused the discrete gel fragments to cement together, resulting in an abrupt increase in lump volume at a much lower temperature, near 500°.

We thank D.S.I.R. for a maintenance grant (to J. F. G.). The electron-optical examination was carried out during the tenure of the Acheson Research Fellowship at Cambridge University (by J. F. G.), and the authors thank Dr. F. P. Bowden for making this examination possible. They thank also Dr. H. P. Rooksby of G.E.C. Research Laboratories, Wembley, for heating the sample of SnO<sub>2</sub> at 1550—1600°C.

WASHINGTON SINGER LABORATORIES, THE UNIVERSITY,  
PRINCE OF WALES ROAD, EXETER.

[Received, August 16th, 1959.]